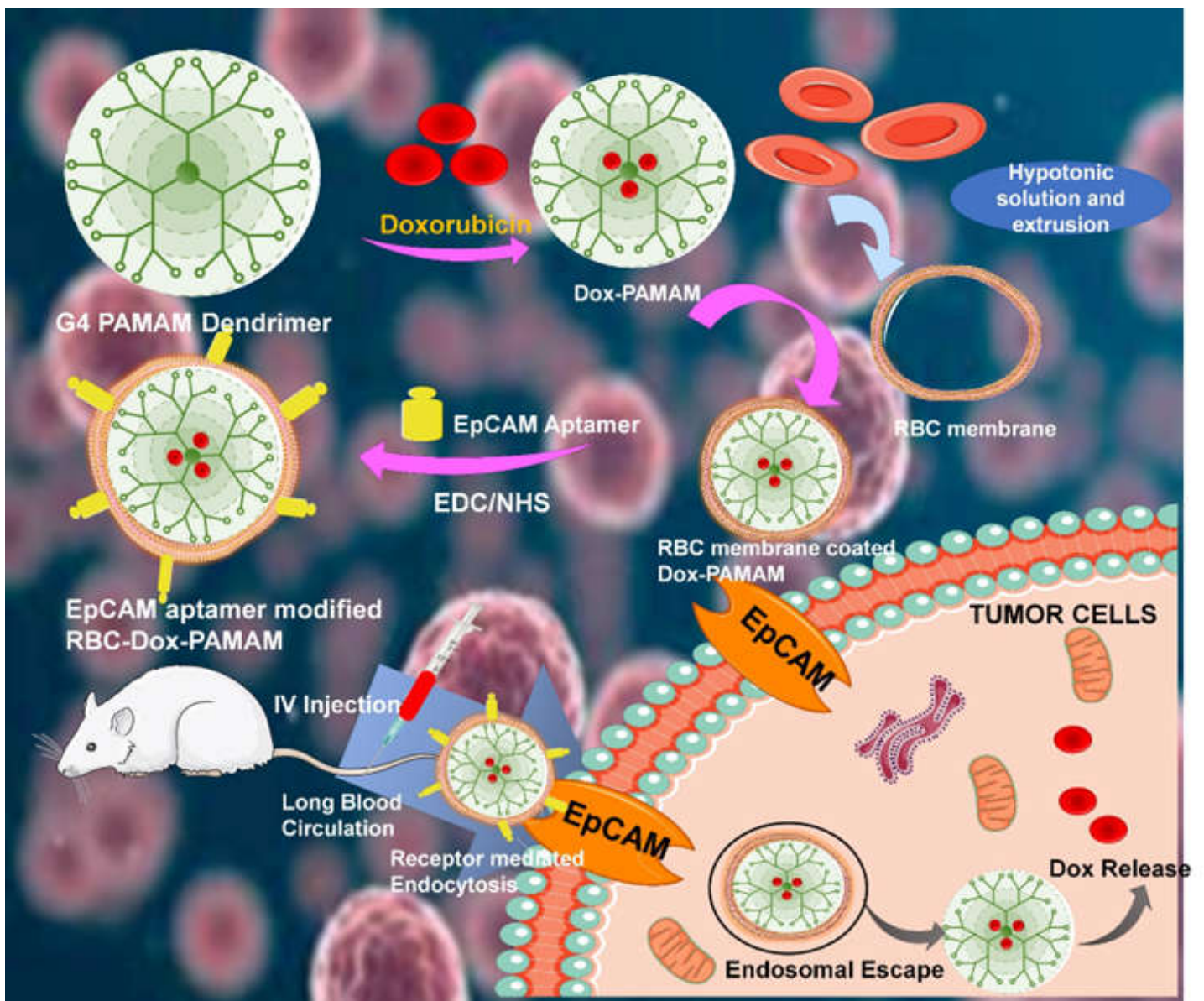


DETAILS OF THE RESEARCH:

TITLE: Aptamer-grafted, cell membrane-coated dendrimer loaded with doxorubicin as a targeted nanosystem against epithelial cellular adhesion molecule (EpCAM) for triple negative breast cancer therapy

Graphical abstract:



Abstract:

The major issue associated with chemotherapeutics is the non-specific distribution, extended range of toxicity, and low intratumoral accumulation. Targeted therapy using aptamers could be a ground-breaking approach in cancer treatment. Poly(amidoamine) PAMAM dendrimers are a type of nanocarriers with a well-defined structure, higher encapsulation efficiency and modification surface groups. However, the toxicity of cationic dendrimers and non-targetability poses a great risk to patients' health. Considering this, we developed a EpCAM aptamer-functionalized, red blood cell (RBC) membrane-camouflaged PAMAM dendrimer loaded with doxorubicin to selectively target EpCAM-positive triple-negative breast cancer (TNBC) cells. An increase in size of doxorubicin (Dox) loaded PAMAM was observed from 11.34nm to 108.4nm post coating with RBC membrane and aptamer, respectively. The biocompatibility and blood circulation time were enhanced by the coating of the RBC membrane on the surface of the dendrimers while functionalization with aptamers improved its cancer cell internalization. The results obtained suggested that the coating with RBC provided controlled and sustained release during the 140 hours of study. *In vitro* cell viability study showed enhanced apoptosis and significantly elevated uptake by the cancer cells as compared with the non-targeted preparation. Furthermore, the volume of the tumor was significantly reduced in groups treated with aptamer-modified, cell membrane-coated dendrimer due to selective internalization in the cancer cells only. This novel, personalized, and targeted therapy could be a potent platform for TNBC therapy.

Keywords: Triple-negative breast cancer; dendrimer; red blood cells; aptamer; EpCAM.

1. Introduction

Breast carcinoma is a mixed ailment rather than a mere homogenous disease. Following this path, identifying subtypes of breast cancers and specific targets to reduce their progression is a potential treatment strategy. Triple-negative breast cancer (TNBC) is one such subtype that is clinically characterized by a lack of progesterone, estrogen, and human epidermal growth factor 2 receptors contributes to its paucity of effective treatment. Reduced overall survival (10.2 months), high relapse rate, and progression-free survival (5-6 months) demonstrate the poor prognosis of TNBC. Chemotherapy is still the mainstay of treatment. Anti-microtubule agents such as taxanes, alkylating agents such as cyclophosphamide and anthracycline or DNA-intercalating agent along with 5-fluorouracil (5-FU) are often what oncologists reach for to treat TNBC [1].

An anthracycline class medication, doxorubicin has been explored for most cancers to date. However, its short half-life and cardiotoxicity confine its therapeutic potential. Despite aforementioned chemotherapeutics, the prognosis of TNBC is highly poor as the antitumor potential of such agents could attain plateau. Consequently, the futuristic framework holds targeted, combination, and gene therapy which could augment therapeutic response in disease subsets. Even though combination therapy and early detection can improve the rate of survival, ground-breaking methods are still required to reduce the associated side effects. Some research is now leaning towards improving the potential of existing drugs by developing novel drug delivery systems. Several nanocarriers have been studied including micelles, liposomes, polymeric drug conjugates, lipoplexes, dendrimers, and inorganic nanoparticles for TNBC [2]. Dendrimers are three-dimensional macromolecular structures comprising a hydrophobic core and hydrophilic branches mimicking a tree [3]. The unique structure exemplifies dendrimers from other investigated nanocarriers and have numerous advantages. The low polydispersity affords astonishingly consistent efficacy, high loading potential, and passive targeting prospect

offered by the size of dendrimer and globular structures which could deliver both hydrophobic and hydrophilic agents, advancing their therapeutic profile [4]. poly(amidoamine) (PAMAM) dendrimer is the first developed class of dendrimer for clinical demonstration. PAMAM has been explored in the drug delivery industry as they can hold poorly soluble drugs inside their vacant cavity while the hydrophilic moieties along with targeting ligands, antibodies, deoxyribose nucleic acid (DNA), or ribonucleic acid (RNA) could be conjugated or attached (whichever is efficient) to the peripheral functional groups. Nanometric size, scalability, and ease of fabrication are some ascendancies that made dendrimers important carriers for numerous therapeutic agents. Our group developed a 3, 4-difluorobenzylidene curcumin (CDF)-loaded hyaluronic acid-coated PAMAM dendrimer to investigate the effect on pancreatic cancer cells. As hyaluronic acid shows a strong propensity towards CD44 receptors, the targeted preparation demonstrated 1.71 times increased half maximal inhibitory concentration (IC₅₀) value as compared with the non-targeted dendrimer. The active targeting ability has also been investigated in numerous research by conjugating ligands such as arginine-glycine-aspartate (RGD) [4], folic acid (FA) [5], biotin [6], human epidermal growth factor receptor-2 (HER-2) [7], aptamers [8], and small interfering RNA (siRNA) [9]. Another study reported the delivery of doxorubicin by attaching it via a succinate linker on a third-generation glucoheptoamidated poly(amidoamine) dendrimers to glioma cells. The results showed significant apoptosis and cell cycle arrest at the G2/M phase. The conjugated system showed 4.5-fold improved anticancer response than with the drug alone, indicating a promising effect of dendrimer in mitigating glioma cells [10].

The cationic nature of dendrimers, however, highly endorses interaction with red blood cells (RBCs), questioning their safety profile. High interaction with dendrimers can rupture the RBC membrane and potentiates cytotoxicity that limits its use [11]. The positioning of natural cell membranes over the surface of chemical therapeutic entities facilitates man-made vectors to

share similar functionalities and merits developed by the nature. Such a revolution transformed the pharmaceutical industry by biomimicking natural human physiology. PEGylation, for example, could enhance the biodistribution of nanoparticles while avoiding immunological response [12]. The swift clearance of dendrimers by the reticulum-endothelium system (RES) and lack of targeting capability would minimize their effective response while increasing serious adverse effects. Hence, structural modification of dendrimers could enhance the blood circulation time with increased accumulation at the site of action. In this regard, dendrimers could be coated with the RBC membrane to improve their flexibility, stability, and biocompatibility. Since RBC membranes express CD47 receptors, they easily undergo phagocytic inhibition of erythrocytes promoted by macrophages. Therefore, coating of RBC membrane on the surface of dendrimers could reduce the RES uptake and improve the blood circulation time. Nanoparticles could be tailored with patient's erythrocyte membrane to avoid the risk of unsolicited immunological response. Considering this, gambogic acid-loaded RBC membrane-coated poly (lactic-co-glycolic acid) (PLGA) nanoparticles were fabricated that accelerated the therapeutic anticancer response in SW480 implanted Balb/c mice [13]. RBC-camouflaged cells could improve the blood circulation time, but the major problem associated is non-targeting potential.

Aptamers are single-stranded oligonucleotide with high binding capacity and selectivity towards targeted cells. Aptamers offer profound benefits over monoclonal antibodies due to high robustness, low immunogenicity, and increased penetration [14]. An aptamer-functionalized drug delivery system could be a revolutionizing approach in cancer treatment, especially for TNBC. The versatility of aptamers enables them to fit into the pockets of targets prompting magnificent binding efficacy.

Epithelial cell adhesion molecule (EpCAM) is a cancer-associated antigen overexpressed on TNBC cells, making it an important target for this malignancy. EpCAM is one of the earliest

identified targets in TNBC. Nonetheless, not much clinical progress has been made to target and mitigate this antigen [15]. In a study, nearly 2 of 3 TNBC cells showed strong expression for the EpCAM oncogenic protein, which is linked to poor prognosis [16]. It has been demonstrated that an EpCAM-functionalized single-walled carbon nanotube (SWCNT) induced higher apoptosis than non-targeted therapy in EpCAM-positive cells for the treatment of breast carcinoma [17].

The development of a highly advanced targeted therapy should emphasize sufficient drug loading, enhanced permeation, elevated biocompatibility, increased circulation, high tumor internalization, and accumulation. Further, the targeted preparation should contain nano-oncotherapeutics. Our targeted therapy was customized to accomplish the primary demand for cancer therapy.

Herein, we developed a targeted RBC membrane-camouflaged drug-loaded PAMAM dendrimers for TNBC therapy. In this study, doxorubicin (Dox) was entrapped within the core of PAMAM dendrimers and then layered with the RBC membrane, making it a biomimetic therapeutic system. Next, the camouflaged drug-loaded nanoparticle was tagged with EpCAM aptamers to selectively deliver to the cells of TNBC only. The efficacy and safety profile were estimated *in vitro* and *in vivo*.

2. Materials and methods

2.1. Materials

4.0G PAMAM dendrimers, 3-[4,5-dimethylthiazol-2-yl]-2,5 diphenyltetrazolium bromide MTT and doxorubicin (Dox) were obtained from Sigma Aldrich. EpCAM aptamer (5'-amino-CAC TAC AGA GGT TGC GTC TGT CCC ACG TTG TCA TGG GGG GTT GGC CTG-3') was obtained from Santa Cruz Biotechnology.

2.2 Development of Dox-loaded PAMAM dendrimers (Dox-PAMAM)

Dox (2mg) was dissolved in 4ml of Dimethyl sulfoxide (DMSO) and allowed to stir overnight in a dark room. Next, the drug solution was added to a vial containing 20mg of 4.0G poly(amidoamine) (PAMAM) and the reaction were carried out for 24 hours. Afterward, phosphate-buffered saline (PBS) was added and extracted with a sufficient quantity of ethyl acetate to remove the free drug. The solution was lyophilized further to obtain dark red preparation of Dox-loaded PAMAM. The encapsulation efficiency (EE%) and drug-loading capacity (DL%) of Dox were determined by spectrophotometric technique at 480nm [18].

2.3 Development of RBC membrane-derived vesicles

The RBC membrane was extracted according to a previously published protocol [19]. Briefly, 5ml of blood was isolated from Balb/c mice (19-23g) and collected in a heparin-filled vacutainer. To separate the RBCs, PBS (3ml) was added to the blood and the mixture was centrifuged at 3000rpm for 5 minutes at 4°C. After removing the serum, the suspension was irrigated with ice-cold PBS several times to remove the buffy coat. Nearly 0.25×PBS was then added to the prepared RBC and again centrifuged at 10,000rpm at 4°C to eliminate hemoglobin and acquire pink-colored ghost pellets of RBC. The RBC ghost was then sonicated in a capped vial for 5 minutes. The RBC membrane was then stored at -80°C post-lyophilization.

2.4 Grafting of Dox-loaded PAMAM dendrimers with RBC membrane (RBC-Dox-PAMAM)

RBC membrane (2mg) was stirred with Dox-PAMAM (4mg) in a vial containing PBS for 2 hours. The solution was then sonicated using a bath sonicator for 10-15 minutes. The RBC membrane was enveloped over PAMAM through electrostatic interaction. The success of coating was ascertained by measuring the size and zeta potential of obtained camouflaged nanoparticulate system [20].

2.5 EpCAM aptamer conjugation of RBC-Dox-PAMAM

The carboxylic acid of EpCAM aptamer was activated using EDC and NHS. 10μl of EDC/NHS solution (2mg in 200μL DNase RNase free water) was stirred with 600μg aptamer in 500μL

water and stirred at 4°C for 3 hours. The resultant solution was filtered to remove excess EDC and NHS. The activated EpCAM aptamer was then added to the solution of RBC-Dox-PAMAM (2mg/ml) and stirred for 24 hours at 4°C. The resultant mixture was centrifuged at 10,000rpm for 15 minutes to remove the unconjugated aptamer.

2.6 Characterization of Dox-PAMAM, RBC-Dox-PAMAM, and Apt-RBC-Dox-PAMAM

The physical state of doxorubicin and Dox-PAMAM was examined using differential scanning calorimetry (DSC) with approximately 5mg of samples heated at a temperature within the range of 40°C-400° with a heating rate of 10°C/min in an aluminum pan under a constant nitrogen flow rate. The Fourier transform infrared spectra of pure drug and Dox-PAMAM were recorded and obtained using Bruker FTIR spectrometer in the region of 400 to 4000cm⁻¹. ¹H NMR spectra of G4 PAMAM dendrimers and Dox-PAMAM were obtained using D₂O water as the solvent at room temperature with 400MHz. MestReNova software was then used to locate and interpret the obtained peaks. The particle size and zeta potential were investigated using dynamic light scattering (DLS) technique. Encapsulation success of doxorubicin was also estimated by the fluorescence spectrometric method using 560nm at λ_{em} and 480nm at λ_{ex} . The morphology of the obtained nanotherapeutic system was examined by transmission electron microscope (TEM) and atomic force microscope (AFM).

2.7 Doxorubicin release profile from the complex

The release profile of doxorubicin was recorded at the pH of blood (i.e., pH 7.4) and the pH of lysosomes (i.e., pH 5.5) using equilibrium dialysis method. The fabricated preparations equivalent to the weight of 10mg was sealed in a dialysis bag, having a molecular weight cut off of nearly 10kDa. The bag was then immersed in beakers containing 50ml of buffer (pH 7.4 and 5.5) and was incubated in an incubator shaker. 1ml of outer phase medium was withdrawn at specific time intervals while simultaneously replacing it with an equivalent amount of buffer

with the same pH as the dialysis medium. The amount of drug release was determined by the spectrometric technique at a predefined time.

2.8 Cell viability assay

To understand the cellular effect of the free drug (Dox), RBC-Dox-PAMAM and Apt-RBC-Dox-PAMAM having an equivalent Dox dose of 0.5µg/ml, 1.5µg/ml, 2.5µg/ml, 5µg/ml and 10µg/ml, MTT assay was executed on 4T1 (EpCAM-positive cell line) and MDA-MB-231 (EpCAM-negative cell line) cells. Primarily, the cells (5000 cells/well) were cultured in a 96-well plate and incubated at 37°C in 5% CO₂. The cells were then treated with the free drug, RBC-Dox-PAMAM or Apt-RBC-Dox-PAMAM for 6 hours. After refreshing the media, the cells were again incubated for 48 hours maintaining 37°C atmospheric conditions. 5mg/ml of MTT solution in PBS (20µL) was then added to each well and incubated further for 4 hours. After aspiration of media, DMSO (100µL) was added further to dissolve the developed formazan crystals. At last, the SpectraMax Ò M2 microplate reader was employed to record the optical absorbance at 570nm, while the 630nm range was used for reference [21].

2.9 Cellular uptake

The uptake ability of targeted and non-targeted RBC-camouflaged doxorubicin-loaded dendrimers was studied. 4T1 cells were seeded at a density of 5×10^4 cells/well and nurtured keeping them undisturbed for 24 hours. The cells were further treated with plain RBC-Dox-PAMAM and Apt-RBC-Dox-PAMAM for 2 hours at 37°C in a serum-free media. Next, the cells were further washed three times with PBS to confiscate extracellular deposits and fixed with 4% paraformaldehyde at 20°C for 20 minutes. The coverslips were then fixed on the slides and scanned using confocal microscope.

2.10 In vivo therapeutic efficacy study

The *in vivo* antitumor study was carried out in female Balb/c mice after approval from the institutional animal ethics committee (IAEC) of Jamia Hamdard (Protocol no. 1734). 4T1 cells

(5×10^5) in PBS (0.1ml) at pH 7.4 was administered subcutaneously to the right flank of female Balb/c mice weighing 19-23g for the development of 4T1 tumor-bearing mice. When the size of the tumors reached 30mm^3 , the animals were randomly divided into a group of 4 ($n=6$) and treated with 200 μL of plain Dox, RBC-Dox-PAMAM or Apt-RBC-Dox-PAMAM (equivalent to 5mg/kg of Dox). All preparations were administered via the tail vein while those that received PBS were kept as negative control. The tumor volume was recorded using the below formula:

$$\text{Tumor volume (mm}^3\text{)} = \text{length} \times \text{width} \times \text{height}/2$$

The weight of the mice along with tumor weight were also recorded to estimate the therapeutic efficacy and desired toxicity of the targeted preparation in comparison to plain drug and non-targeted therapy [22].

2.11 Pathological evaluation of systemic toxicity

Thirty days post-treatment with Apt-RBC-Dox-PAMAM, RBC-Dox-PAMAM, plain Dox or PBS, the mice were euthanized and the systemic toxicity on major vital organs was observed. On such note, heart, liver, kidney, spleen, and tumors were isolated, irrigated with PBS, and fixed with 10% formalin solution. The tissues were entrenched afterwards in paraffin and stained with hematoxylin and eosin (H&E) to obtain images under 40x using an inverted optical microscope [22].

2.12 Statistical analysis

The results of the quantitative analysis of the study data, which were collected in triplicate, were expressed as mean and standard deviation (SD). One-way analysis of variance (ANOVA) was used in the statistical analysis, which was carried out using the GraphPad prism. A p-value of 0.05 or less was regarded as statistically significant.

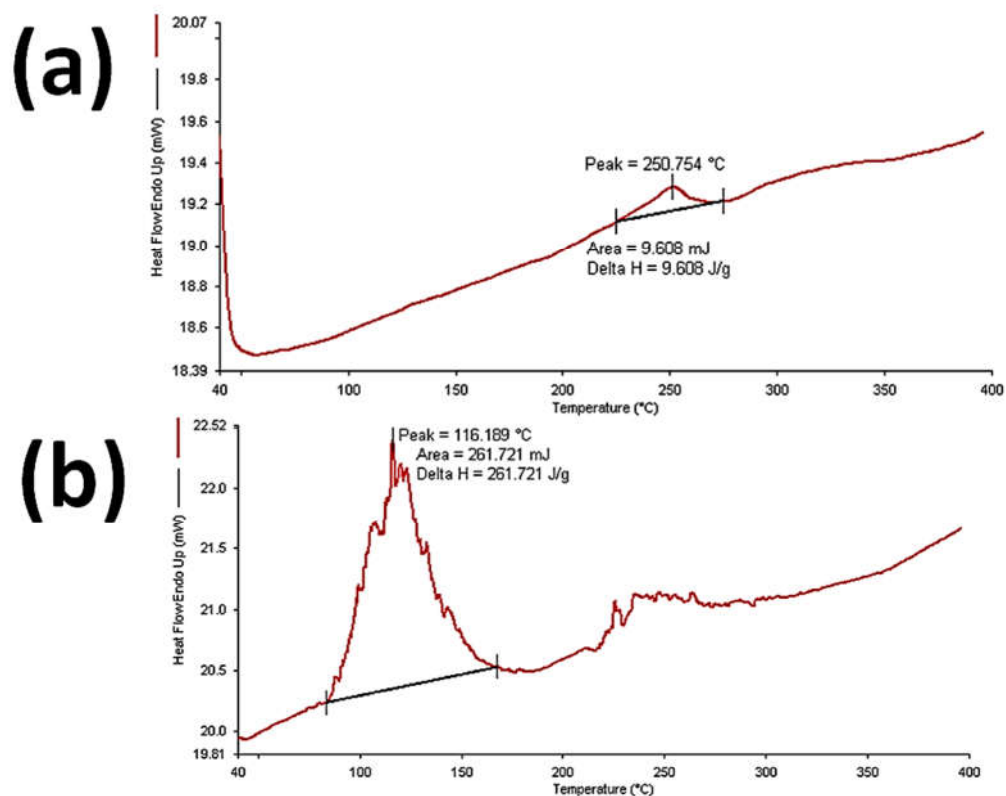


Figure 1: Differential scanning calorimetric analysis of Dox (a) and Dox-PAMAM (b).

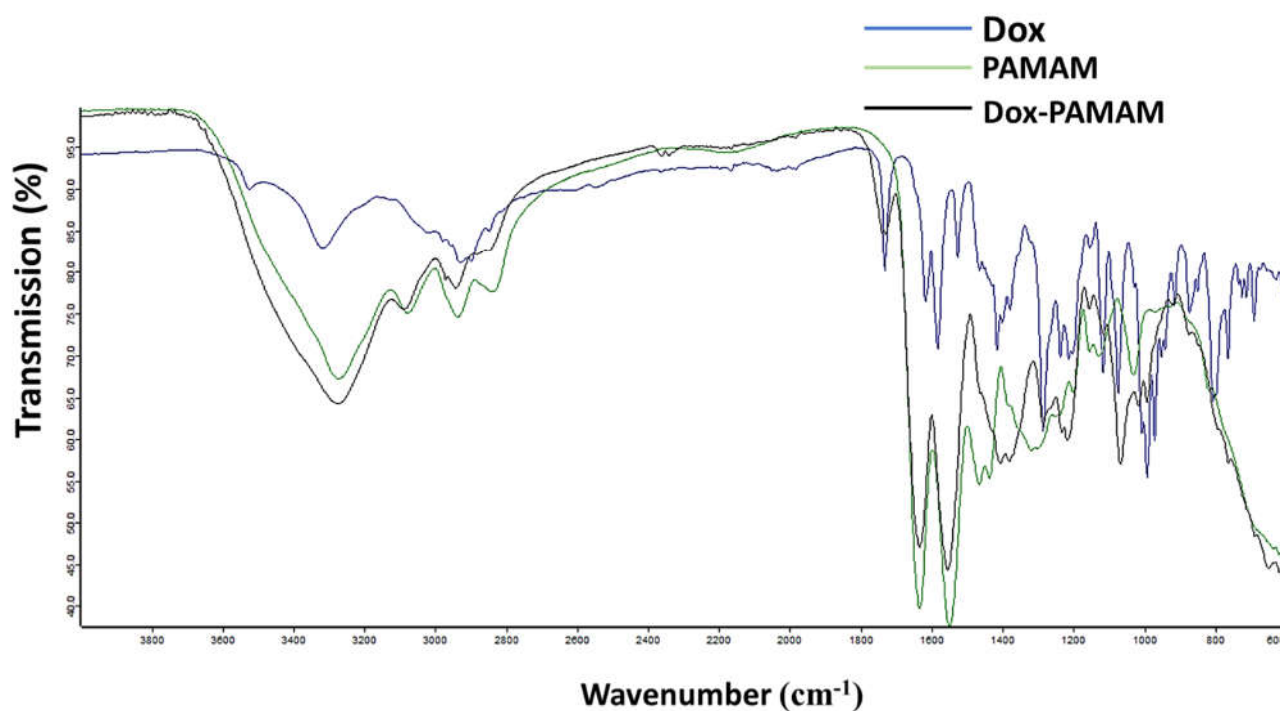


Figure 2: Fourier transform spectroscopic study of Dox, PAMAM and Dox-PAMAM

3. Result and discussion

3.1 Development and characterization of Dox-PAMAM

The PAMAM dendrimer is a highly organized globular-shaped structure known for its potential to encapsulate hydrophobic compounds inside the core. Doxorubicin is a hydrophobic compound with subtherapeutic efficacy despite DNA-intercalating properties. Moreover, low absorption and high rate of elimination limits its clinical use. Hence, we employed PAMAM dendrimers to entrap doxorubicin to expand its therapeutic window. The encapsulated entities demonstrate the presence, absence, or relocation of peaks owing to the alteration in a crystalline lattice, boiling sublimation, or melting point providing information related to the quantitative and qualitative information of molecular entities residing inside the complex structures. The DSC thermogram of pure doxorubicin showed an endothermic peak at 250.75°C. The elimination of such peak in doxorubicin-loaded PAMAM dendrimers confirms excellent drug encapsulation (Figure 1 a and b) [23]. The absorption peaks of pure-drug doxorubicin and Dox-PAMAM obtained by fourier-transform infrared (FTIR) spectrometer are shown in Figure 2. Doxorubicin showed characteristic peaks at 3525 and 3316 cm^{-1} , which are accredited to O-H and N-H stretching vibrational groups. The C=O group showed stretching vibration at 1727 cm^{-1} , confirming the purity of drug. The G4 PAMAM dendrimers showed characteristic absorption bands at 3301 cm^{-1} , 3077 cm^{-1} , and 1248 cm^{-1} which are attributed to N-H stretching vibrations of amines, antisymmetric vibration of primary substituted amine and C-H stretching, while peaks at 1547 cm^{-1} , 1463 cm^{-1} , 1316 cm^{-1} is due to N-H bending of substituted amine. The peak at 1125 cm^{-1} is due to C-C bending of PAMAM dendrimers. In Dox-PAMAM spectra, an upshift of C=O stretch of doxorubicin is observed, which indicates the conformational change in the appearance of drug. The major characteristic peaks are of G4 PAMAM dendrimers evidenced by the incorporation of the drug inside the core of dendrimer. Thus, the spectra obtained by FTIR have been offset for simplicity [24–26]. The ^1H NMR spectra of the

dendrimers and the formulation are represented in Figure 3. The intensified peak at 3.5ppm corresponds to the methylene protons 'd'. The triplet peaks at a and c are assigned at 2.8ppm and 3.4ppm, respectively, which is due to the presence of CH₂ protons. The doublet peak at 2.6ppm is assigned to b, which is due to CH₂/N-H protons. In the formulation, only peaks c and c are observed (Figure 3a and b) [27]. According to the literature, doxorubicin shows a peak at 7.54ppm and 7.70ppm [28], which were not observed in the spectra of Dox-PAMAM (data not shown), suggesting the successful encapsulation of the drug. To confirm the encapsulation of doxorubicin in PAMAM dendrimers, a fluorescent spectroscopic study was performed. Plain Dox showed a peak at 560nm while no such peak was present at such wavelength indicating the successful encapsulation of drug inside the core. Our results are consistent with the other published studies (Figure 3c) [9].

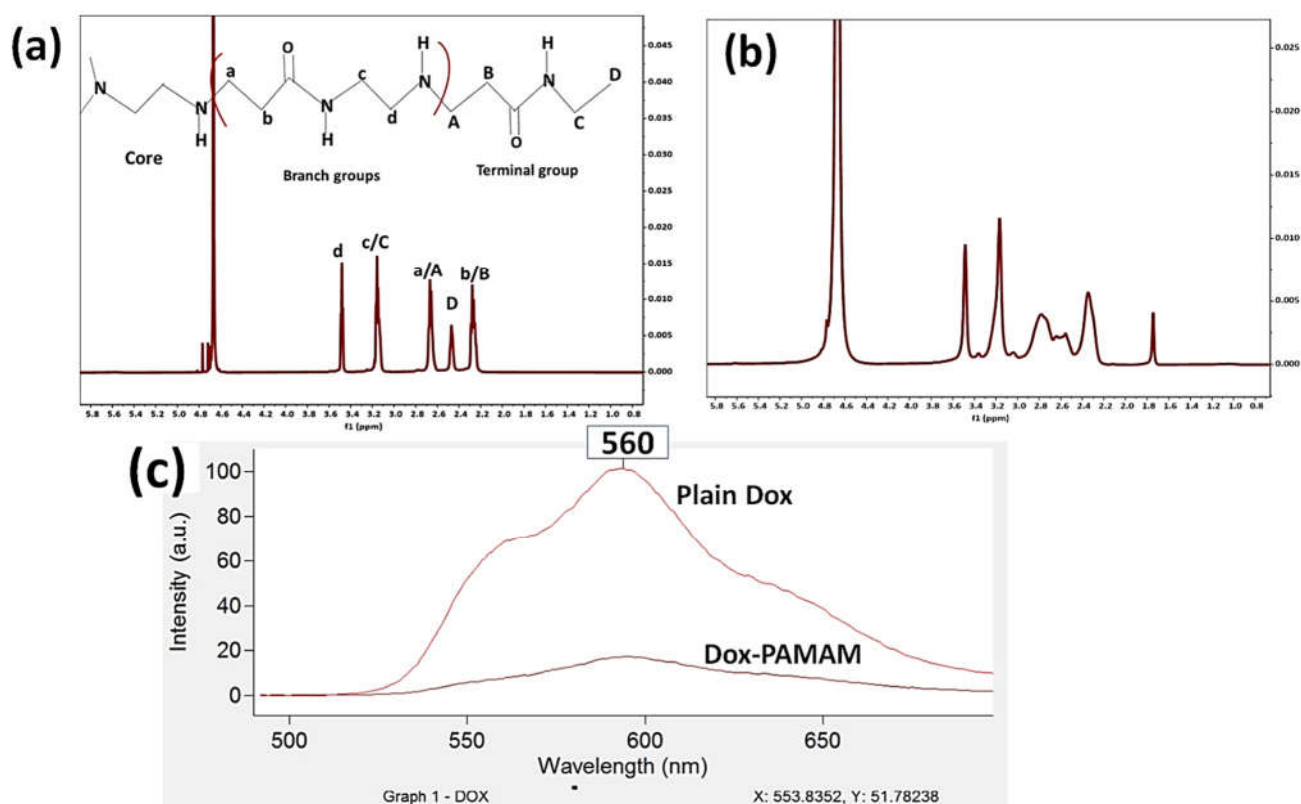


Figure 3: Nuclear magnetic resonance-based analysis of PAMAM (a) and PAMAM-Dox (b); fluorescence spectroscopic study of Dox and Dox-PAMAM.

TEM and AFM images of RBC-Dox-PAMAM and Apt-RBC-Dox-PAMAM are shown in figure 4 suggesting that the grafted aptamer on RBC-camouflaged nanoparticle are of spherical shape. Our results are consistent with the previously published studies [29,30].

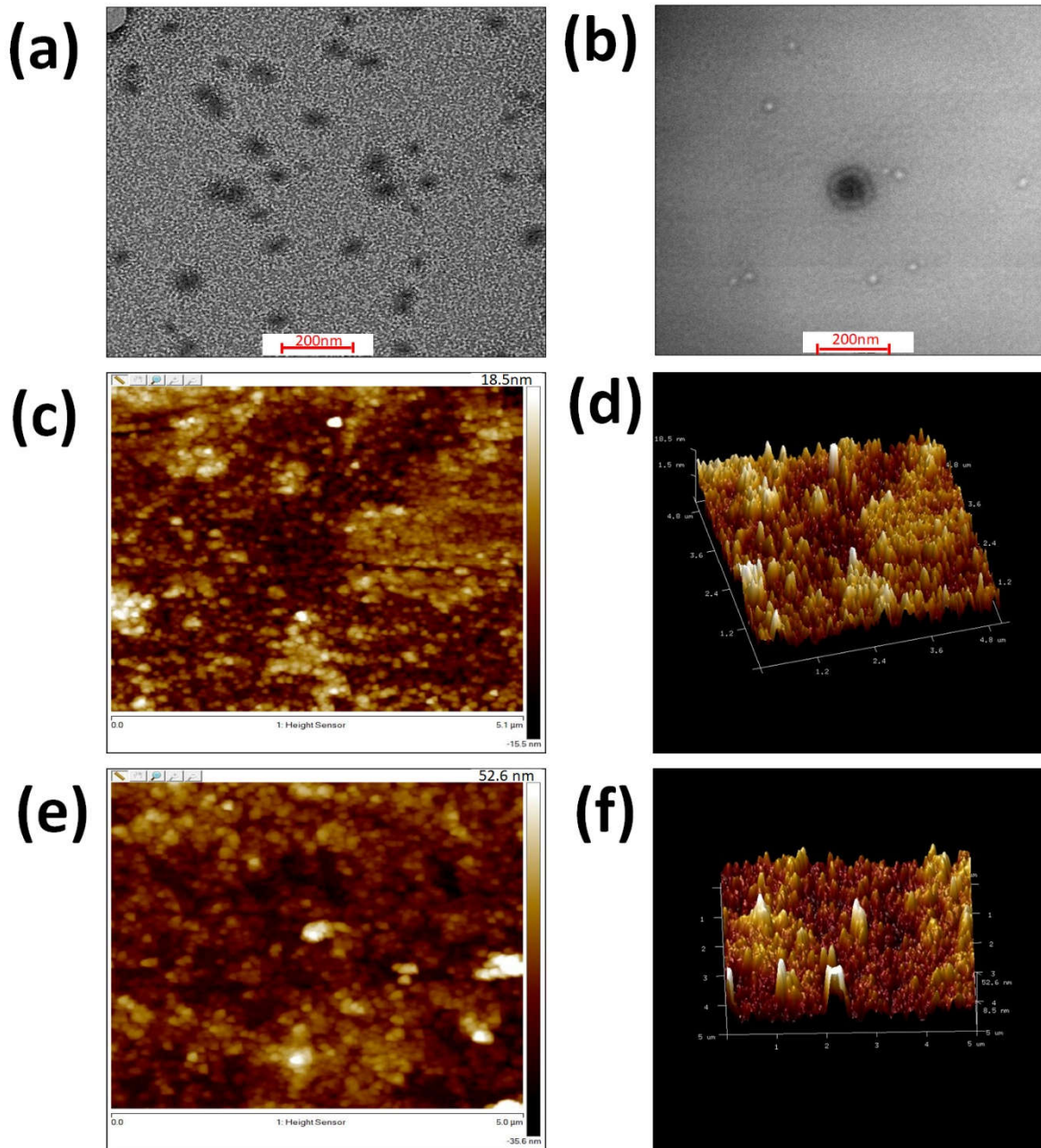


Figure 4: Transmission electron microscopic images of Dox-PAMAM (a) and RBC-Dox-PAMAM (b); atomic force microscopic images of Dox-PAMAM (2D and 3D) (c and d) and RBC-Dox-PAMAM 2D and 3D) (e and f)

3.1.2 Drug loading and encapsulation efficiency

The drug loading and encapsulation efficiency was investigated through spectromic analysis. The loading percentage of Dox was obtained to be $37\pm 71\%$ while the encapsulation efficiency was $57.12\pm 4.4\%$. Our result is in accordance with the previously published results [31].

3.2 Development of RBC membrane-camouflaged Dox-PAMAM

The RBC membrane was isolated from freshly collected blood to envelop the Dox-PAMAM and develop a nano-oncotherapeutic platform with extended biocompatibility. Since RBC membranes express CD47 glycoprotein, they are easily uptaken by phagocytosis. Thus, coating the membrane by electrostatic interaction on PAMAM dendrimers could improve the pharmacokinetic profile. DLS results revealed the size of Dox-PAMAM to be 11.34nm which increased up to 75nm. A further increase in size was reported after conjugation with the aptamer (108.4nm). Moreover, after coating with the RBC membrane, the zeta potential changed from 17.17mV to 1.081mV confirming the successful coating of the membrane. A further decrease in zeta potential of up to -26.53mV was seen, indicating the conjugation of aptamer on surface of RBC-camouflaged PAMAM dendrimer (Figure 5).

3.3 Doxorubicin release profile from the complex

The *in vitro* release profile of Dox from Dox-PAMAM and RBC-Dox-PAMAM was evaluated at different time intervals and at different pH. Since the pH of cancer cells is slightly acidic, it becomes necessary to accurately inspect the behavior or pattern of drug release at varying pH levels, especially while dealing with the targeted preparations. Alibolandi et al found no significant difference in the release profile of gemcitabine from nanoparticles, and aptamer decorated nanoparticles, as aptamers alone, do not affect the rate of drug release but rather promotes cell uptake and internalization, providing supreme therapeutic results [32]. As illustrated in figure 6, the RBC-coated preparation showed a maximum of 11.58% Dox release at pH 7.4 during 60 hours of study while 58.27% and 49.23% release of Dox was detected from RBC-Dox-PAMAM and Dox-PAMAM, respectively, at pH 5.5 during the 60 hours of study.

A sustained release profile of Dox at physiological conditions is ascribed to the entrapment of Dox in the core of the PAMAM dendrimer. Under acidic conditions, the RBC-camouflaged system demonstrated an accelerated release pattern due to repulsive forces between the protonated $-NH_2$ group of RBC proteins and the surface of the PAMAM dendrimer, causing the detachment of the RBC membrane in presence of hydrogen ions. The inner terminal amino groups of PAMAM, protonates at acidic pH causing charge repulsion. The dendrimer adopts an "extended conformation" as a result. It is important to mention that RBCs acted as a gatekeeper for controlling the release rate, as a lower release rate of the drug was observed as compared with the uncoated Dox-P platform. This system would therefore be efficient *in vivo* due to greater release at the desired site [33].

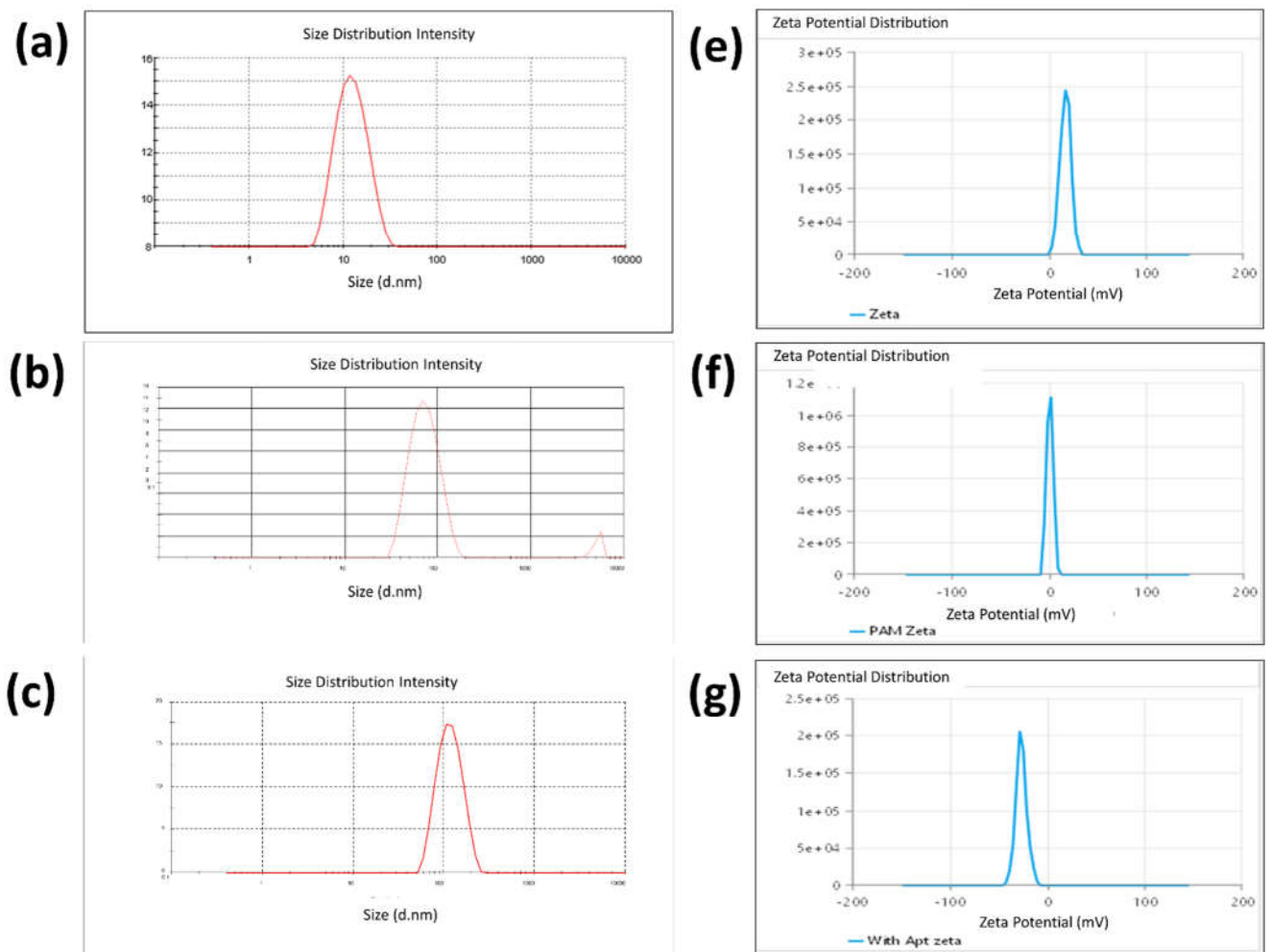


Figure 5: Representation of particle size and zeta potential of Dox-PAMAM (a, e), RBC-coated Dox-PAMAM (b, f) and aptamer-functionalized RBC-coated Dox-PAMAM (c, g)

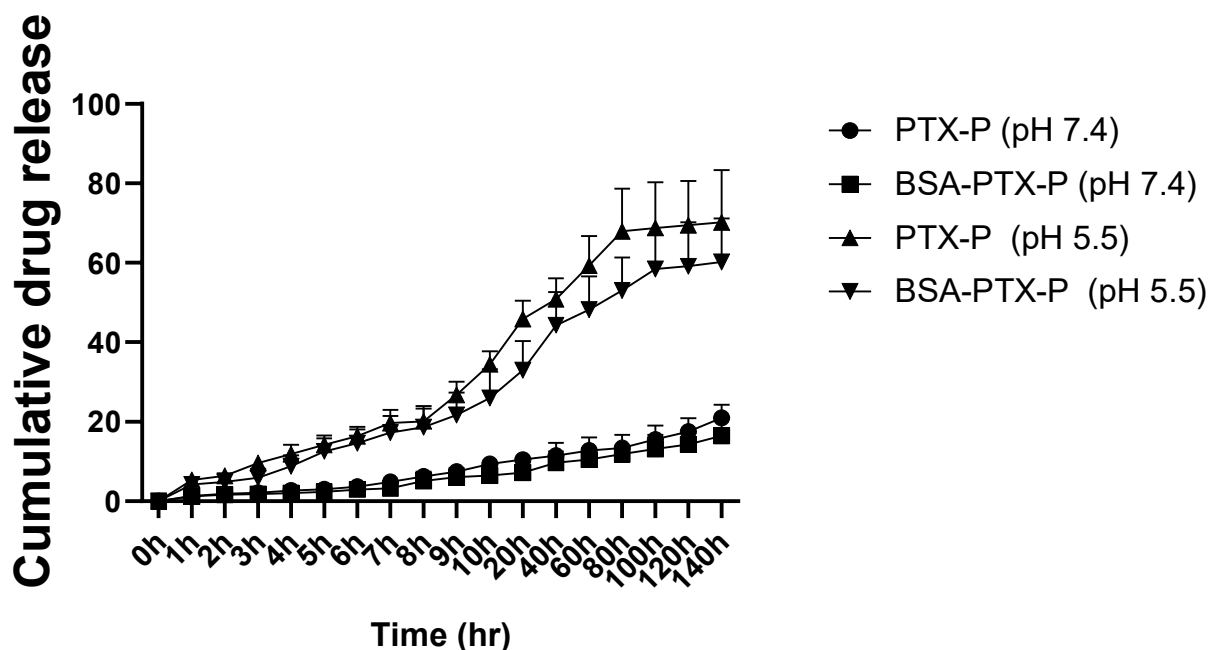


Figure 6: Drug release profile of Dox-PAMAM and RBC-Dox-PAMAM at pH 7.4 and 5.5.

3.4 Cell viability assay

MTT analysis illustrated the viability of cells upon treatment with plain Dox, RBC-Dox-PAMAM or Apt-RBC-Dox-PAMAM on (EpCAM⁺) and MDA-MB-231 (EpCAM⁻) cells. According to the data represented in figure 7a and b, plain doxorubicin exhibited higher toxicity than targeted and non-targeted preparations. Nevertheless, a higher cytotoxic effect was significantly discerned by Apt-RBC-Dox-PAMAM in comparison with RBC-Dox-PAMAM in the EpCAM-positive cell line ($p < 0.05$). Such an augmented effect by the EpCAM aptamer-functionalized biomimetic preparation is due to their selectivity towards specific receptors, causing receptor-mediated endocytosis. The higher binding ability of the aptamer towards EpCAM receptors illustrated efficacious results that spared the healthy cells from the deleterious impact of the cytotoxic substance. In MDA-MB-231 cells, the targeted nano-preparation failed to demonstrate a profound cell-killing effect which is due to non-selectivity towards such cells (Figure 7b). When comparing targeted and non-targeted RBC-coated

PAMAM, doxorubicin showed higher cytotoxicity, which could be due to greater and faster cellular transportation via diffusion rather than following the receptor-mediated cellular internalization.

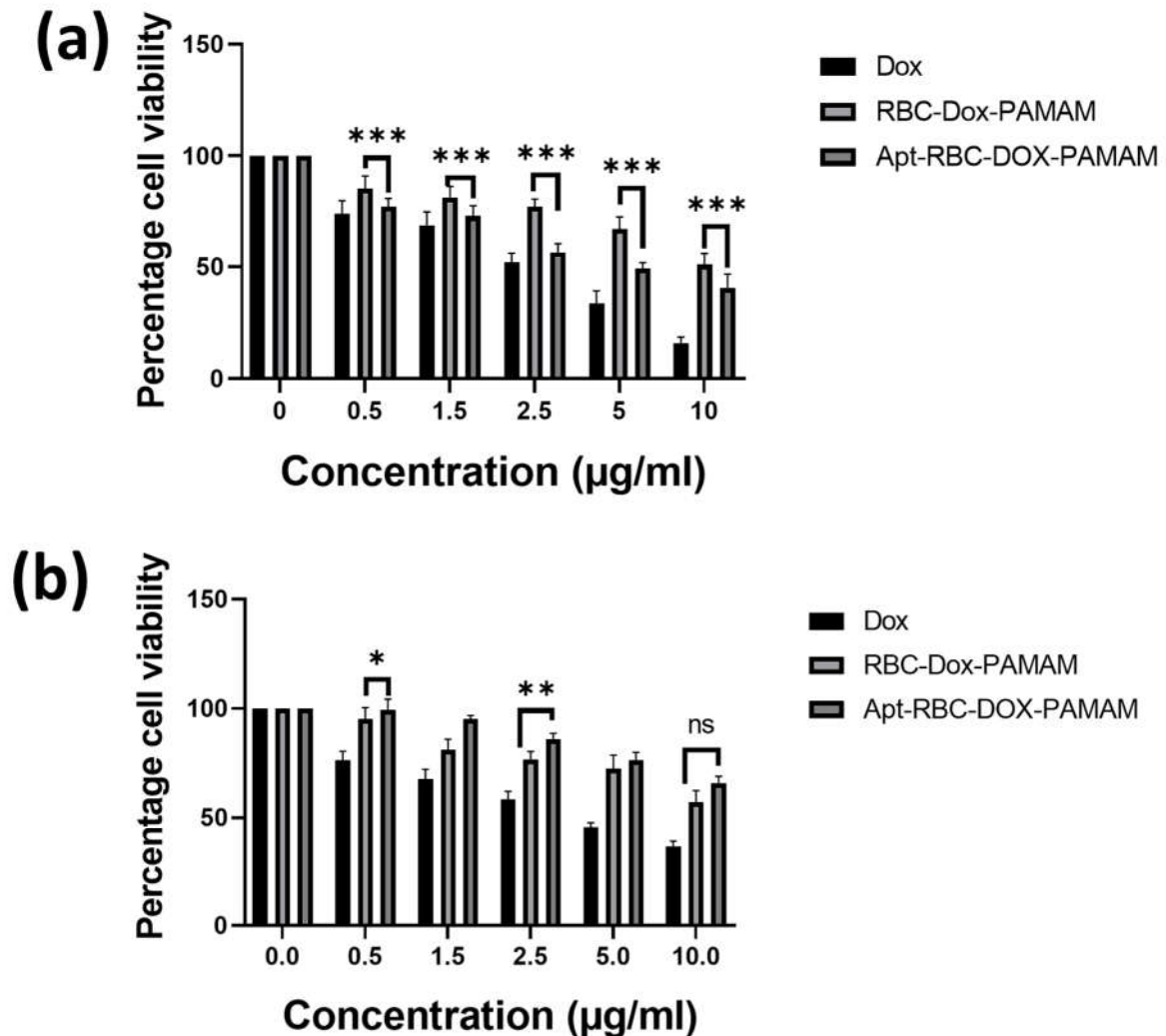


Figure 7: Cell viability study of Dox, RBC-Dox-PAMAM and Apt-RBC-Dox-PAMAM using EpCAM-positive 4T1 cell line (a) and EpCAM-negative MDA-MB-231 cell line for 48 hours (b) [**, *** and ns represents $p < 0.05$, $p < 0.001$ and non-significant, respectively].

3.5 Cellular uptake study

The preeminent feature of targeted therapy is high specificity towards the receptors overexpressed on cancer cells. Herein we evaluated the cellular internalization potential of targeted and non-targeted therapy in 4T1 cells. Hoechst 33342 was used to stain the nuclei

while Dox internalization was seen by the fluorescent property of Dox. The result in figure 8 shows a higher internalization of doxorubicin after 2 hours, while minimal fluorescence was exhibited by the untargeted preparation. An enhanced red fluorescence in the merged section shows a higher accumulation of aptamer-functionalized therapy which is due to receptor-based endocytosis. Similar results were obtained previously exemplifying the role of aptamers in targeted therapy [34,35].

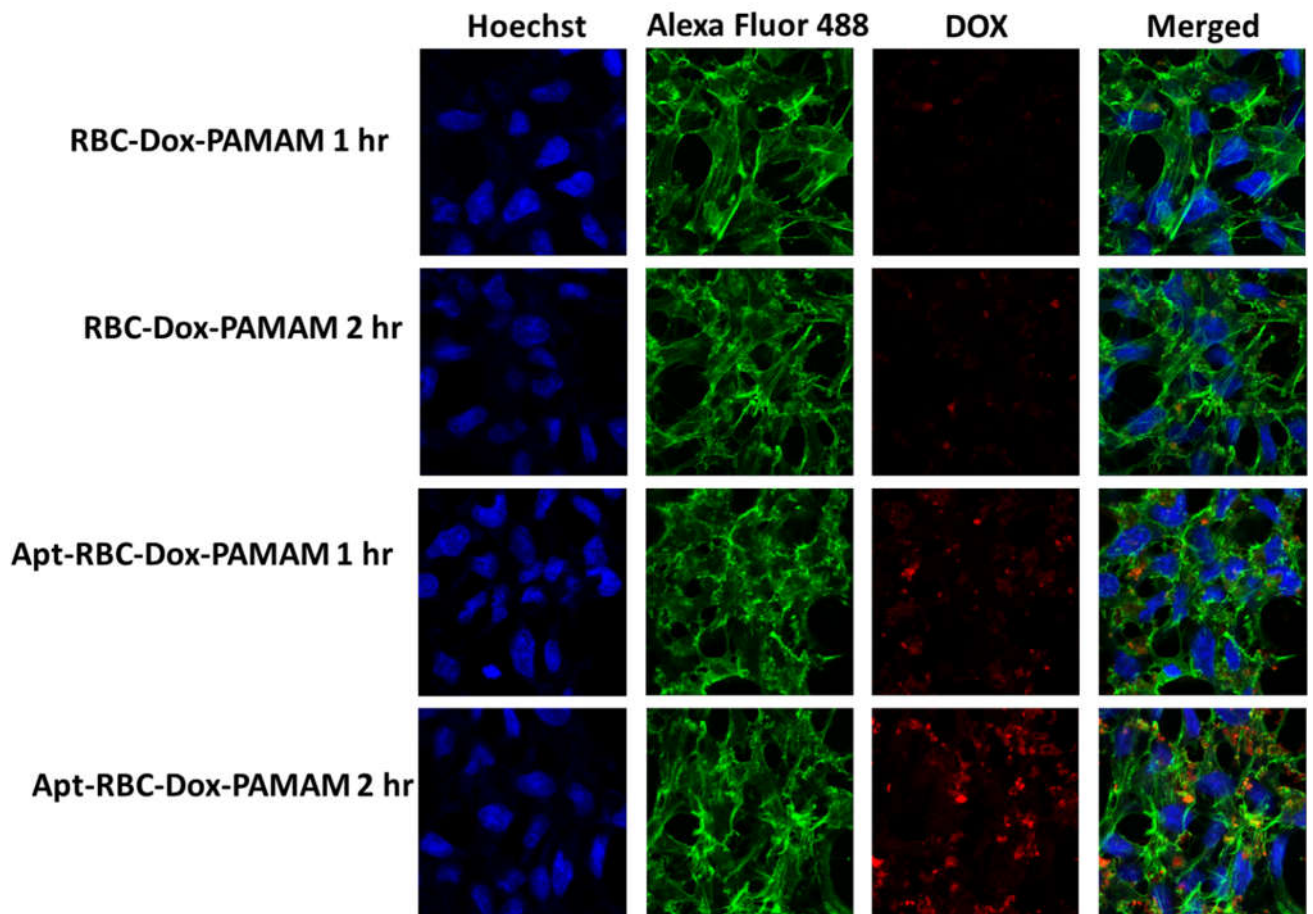


Figure 8: Cell uptake study of RBC-Dox-PAMAM (non-targeted) and Apt-RBC-Dox-PAMAM (targeted) using a confocal microscope

3.6 In vivo therapeutic efficacy study

A comprehensive analysis of the therapeutic potential in terms of tumor volume, body weight loss of the drug, aptamer-mediated targeted therapy, and non-targeted therapy was performed

on 4T1-laden Balb/c mice receiving 5mg/kg equivalent amount of Dox. An appreciable tumor inhibitory effect was observed by the formulations as compared with the free drug. An elevated effect of RBC-Dox-PAMAM on tumor-bearing mice model over those treated with free drug owes to the enhanced permeation and retention (EPR) effect leading to higher accumulation of therapeutic cargo. The coating of RBC membrane on PAMAM dendrimers extended the circulation time that delayed the early clearance of the drug from the bloodstream. A superior tumor inhibitory effect of Apt-RBC-Dox-PAMAM over non-targeted therapy was observed, which is due to higher internalization through receptor-mediated endocytosis. The selectivity of EpCAM aptamer towards EpCAM-positive tumor cells also facilitated improved tumor residence time, decreasing its extravasation. Note that most of the cancer cells failed to show effective results due to resistance to certain chemotherapy. The reason could be tumor heterogeneity or Pg-p efflux. The receptor-mediated response could overcome such hurdles by escaping endosomal uptake. All such stated responsible features improved the therapeutic potential of aptamer-based therapy over non-targeted therapy (Figure 9a and b).

We further examined the treatment's toxicity and safety by analyzing the effect on body weight loss (Figure 9c). No considerable weight loss was observed post-administration of treatment with targeted preparation that confirmed its non-toxicity, adequate dosage, and safe treatment regimen. Such a finding confirms the enhanced therapeutic response of aptamer-functionalized drug delivery systems. Figure 9d demonstrates the tumor weight of mice after treatment, confirming that Apt-RBC-Dox-PAMAM has superior tumor suppressive effect *in vivo*.

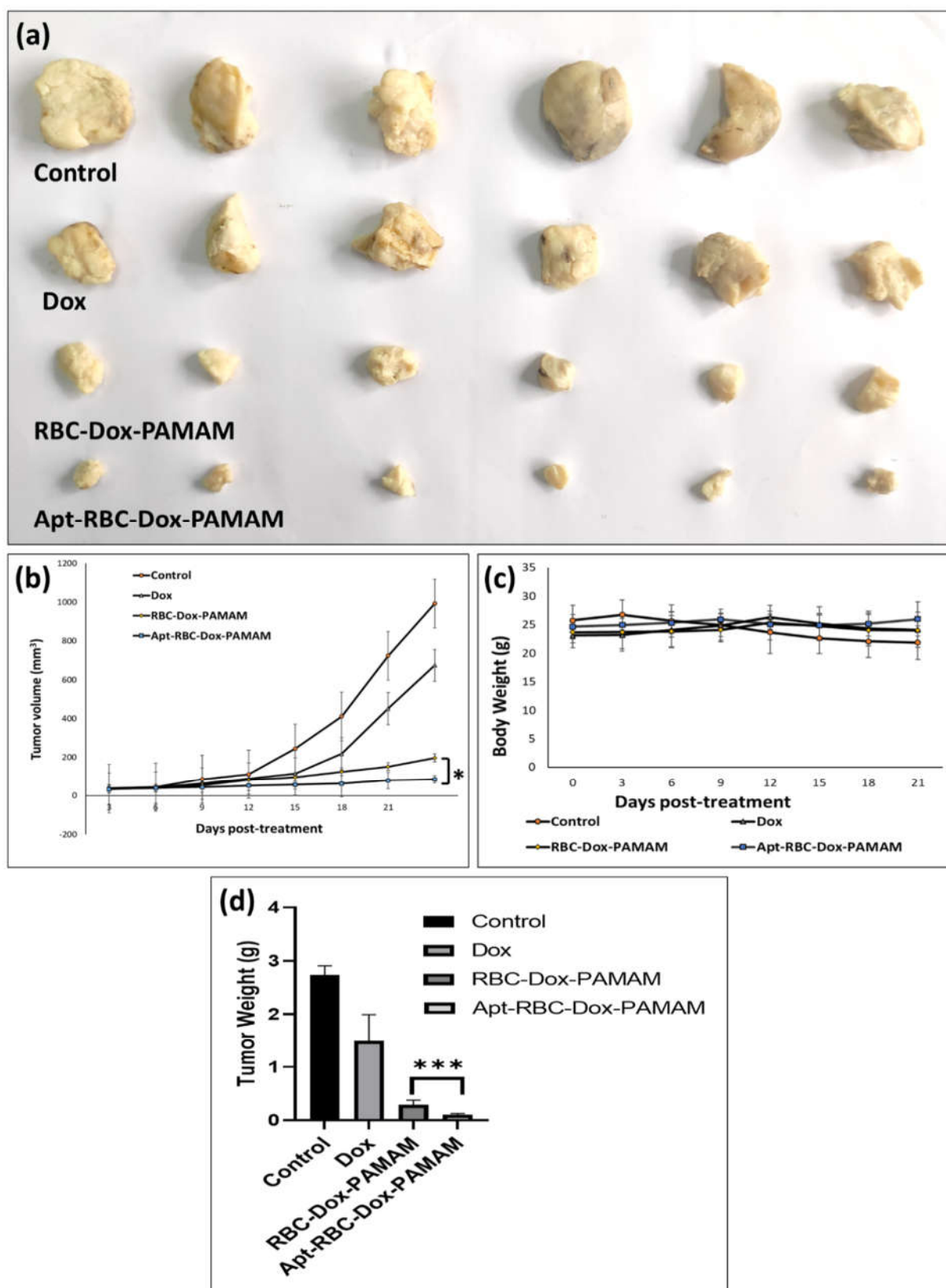


Figure 9: Antitumor efficacy of Apt-RBC-Dox-PAMAM in 4T1-bearing mice model. Pattern of tumor growth in 4T1-bearing mice model (a and b) receiving in intravenous dose of Dox, RBC-Dox-PAMAM and Apt-RBC-Dox-PAMAM; representation of changes in the body weight in 4T1-tumorized mice model post-treatment with Dox, RBC-Dox-PAMAM and Apt-RBC-Dox-PAMAM (c), tumor weight of mice post-treatment with various samples (d) [* represents $p < 0.05$, *** represents $p < 0.001$].

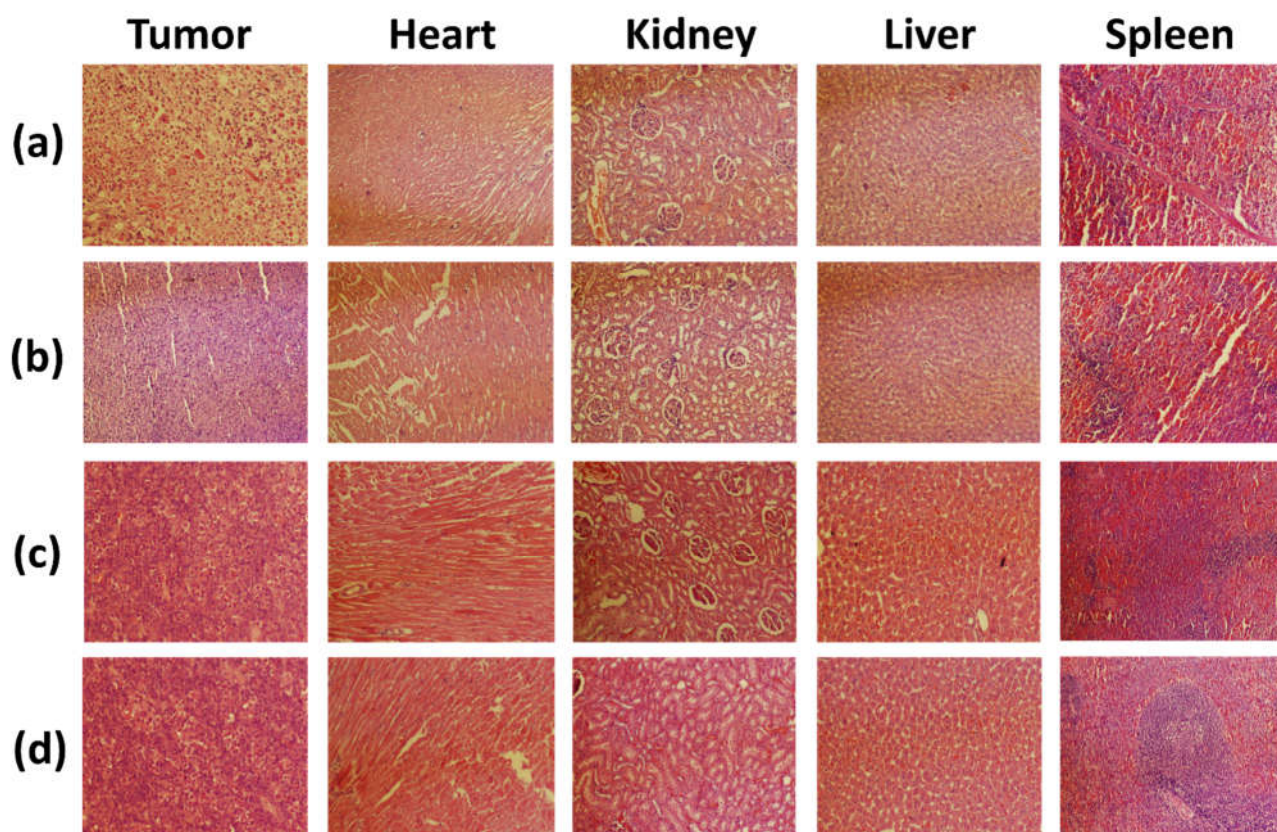


Figure 10: Representation of hematoxylin and eosin-stained tissue of major organ and tumor tissue of 4T1-laden mice post-treatment with control (a), Dox (b), RBC-Dox-PAMAM (c) and Apt-RBC-Dox-PAMAM (d).

3.7 Pathological evaluation of systemic toxicity

Nanotechnology has paved the way in cancer treatment; however, it can affect the physiology of normal cells as well lead to increased toxic effects and organ failure. To overcome such issues, targeted drug delivery systems came into the limelight promoting selective uptake by the tumor cells only without affecting the normal cells. Aptamer-based targeted therapy potentiated increased uptake which resulted in a higher accumulation of drug at the site of action. Apart from therapeutic response, the success of therapy is also a response to its non-toxic effects on vital organs. To establish this, major organs on mice were extracted and pathological alterations of tumors and organs were examined (Figure 10). A high degree of tumor necrosis was observed in mice treated with Apt-RBC-Dox-PAMAM in comparison to those treated with non-targeted therapy and plain Dox, indicating a superior anticancer effect.

High chromatin ratio and large nuclei were observed in the group treated with plain drug and PBS, demonstrating the cell proliferation capability of cancer cells. It is worth mentioning here that, the heart tissue of mice showed severe pathological injuries after treatment with free Dox; however, no histological alterations were reported in those treated with RBC-Dox-PAMAM and Apt-RBC-Dox-PAMAM. This is due to the EPR effect and cell response to non-targeted and targeted preparations, confirming the success of therapy when delivered via PAMAM dendrimers [36].

4. Conclusion

In summary, we developed a cell membrane-camouflaged nano-oncotherapeutic system by coating Dox-loaded PAMAM dendrimers with the RBC membrane. To improve the tumor selectivity and cellular internalization, an EpCAM aptamer was conjugated on the surface of RBC-Dox-PAMAM. The enveloped novel drug delivery system improved the blood circulation time while sensitizing the EpCAM-positive tumor cells to onco-therapeutics to provide the utmost therapeutic effect. The *in vivo* investigation on 4T1-laden tumor mice model demonstrated a significant tumor suppressive effect. The results obtained suggested that the developed targeted biomimetic therapy could improve the clinical outcome and survival of mice with TNBC.

5. Ethics statement

The *in vivo* antitumor study was carried out in female Balb/c mice after approval from the institutional animal ethics committee (Protocol no. 1734).

7. Reference

- [1] K.A. Won, C. Spruck, Triple-negative breast cancer therapy: Current and future perspectives (Review), *Int. J. Oncol.* 57 (2020) 1245. <https://doi.org/10.3892/IJO.2020.5135>.
- [2] A. Sneider, R. Jadia, B. Piel, D. VanDyke, C. Tsiros, P. Rai, Engineering Remotely Triggered Liposomes to Target Triple Negative Breast Cancer, *Oncomedicine*. 2 (2017) 1. <https://doi.org/10.7150/ONCM.17406>.
- [3] P. Kesharwani, R.K. Tekade, N.K. Jain, Dendrimer generational nomenclature: The need to harmonize, *Drug Discov. Today*. 20 (2015). <https://doi.org/10.1016/j.drudis.2014.12.015>.
- [4] A. Sheikh, S. Md, P. Kesharwani, RGD engineered dendrimer nanotherapeutic as an emerging targeted approach in cancer therapy, *J. Control. Release*. 340 (2021) 221–242.

- <https://doi.org/10.1016/J.JCONREL.2021.10.028>.
- [5] S. Wen, H. Liu, H. Cai, M. Shen, X. Shi, Targeted and pH-responsive delivery of doxorubicin to cancer cells using multifunctional dendrimer-modified multi-walled carbon nanotubes, *Adv. Healthc. Mater.* 2 (2013) 1267–1276. <https://doi.org/10.1002/adhm.201200389>.
 - [6] H. Yao, J. Ma, Dendrimer-paclitaxel complexes for efficient treatment in ovarian cancer: Study on OVCAR-3 and HEK293T cells, *Acta Biochim. Pol.* 65 (2018) 219–225. https://doi.org/10.18388/abp.2017_2331.
 - [7] J.B. Otis, H. Zong, A. Kotylar, A. Yin, S. Bhattacharjee, H. Wang, J.R. Baker, S.H. Wang, Dendrimer antibody conjugate to target and image HER-2 overexpressing cancer cells, *Oncotarget.* 7 (2016) 36002–36013. <https://doi.org/10.18632/oncotarget.9081>.
 - [8] H. Dong, L. Han, J. Wang, J. Xie, Y. Gao, F. Xie, L. Jia, In vivo inhibition of circulating tumor cells by two apoptosis-promoting circular aptamers with enhanced specificity, *J. Control. Release.* 280 (2018) 99–112. <https://doi.org/10.1016/j.jconrel.2018.05.004>.
 - [9] M. Ghaffari, G. Dehghan, B. Baradaran, A. Zarebkohan, B. Mansoori, J. Soleymani, J. Ezzati Nazhad Dolatabadi, M.R. Hamblin, Co-delivery of curcumin and Bcl-2 siRNA by PAMAM dendrimers for enhancement of the therapeutic efficacy in HeLa cancer cells, *Colloids Surfaces B Biointerfaces.* 188 (2020) 110762. <https://doi.org/10.1016/j.colsurfb.2019.110762>.
 - [10] J. Czarnik-Kwaśniak, K. Kwaśniak, K. Tutaj, I. Filiks, Ł. Uram, M. Stompor, S. Wołowicz, Glucoheptoamidated polyamidoamine PAMAM G3 dendrimer as a vehicle for succinate linked doxorubicin; enhanced toxicity of DOX against grade IV glioblastoma U-118 MG cells, *J. Drug Deliv. Sci. Technol.* 55 (2020) 101424. <https://doi.org/10.1016/j.jddst.2019.101424>.
 - [11] M. K, K. S, P. N, L. V, P. D, Dendrimers in drug delivery and targeting: Drug-dendrimer interactions and toxicity issues, *J. Pharm. Bioallied Sci.* 6 (2014) 139–150. <https://doi.org/10.4103/0975-7406.130965>.
 - [12] C.M.J. Hu, R.H. Fang, B.T. Luk, L. Zhang, Polymeric nanotherapeutics: Clinical development and advances in stealth functionalization strategies, *Nanoscale.* 6 (2014) 65–75. <https://doi.org/10.1039/C3NR05444F>.
 - [13] Z. Zhang, H. Qian, M. Yang, R. Li, J. Hu, L. Li, L. Yu, B. Liu, X. Qian, Gambogic acid-loaded biomimetic nanoparticles in colorectal cancer treatment, *Int. J. Nanomedicine.* 12 (2017) 1593. <https://doi.org/10.2147/IJN.S127256>.
 - [14] A. Sheikh, P. Kesharwani, An insight into aptamer engineered dendrimer for cancer therapy, *Eur. Polym. J.* 159 (2021) 110746. <https://doi.org/10.1016/J.EURPOLYMJ.2021.110746>.
 - [15] G. Gastl, G. Spizzo, P. Obrist, M. Dünser, G. Mikuz, Ep-CAM overexpression in breast cancer as a predictor of survival, *Lancet (London, England).* 356 (2000) 1981–1982. [https://doi.org/10.1016/S0140-6736\(00\)03312-2](https://doi.org/10.1016/S0140-6736(00)03312-2).
 - [16] A. Gilboa-Geffen, P. Hamar, M.T.N. Le, L.A. Wheeler, R. Trifonova, F. Petrocca, A. Wittrup, J. Lieberman, Gene knockdown by EpCAM aptamer-siRNA chimeras suppresses epithelial breast cancers and their tumor-initiating cells, *Mol. Cancer Ther.* 14 (2015) 2279–2291. <https://doi.org/10.1158/1535-7163.MCT-15-0201-T/85497/AM/GENE-KNOCKDOWN-BY-EPCAM-APTAMER-SIRNA-CHIMERAS>.
 - [17] M. Mohammadi, Z. Salmasi, M. Hashemi, F. Mosaffa, K. Abnous, M. Ramezani, Single-walled carbon nanotubes functionalized with aptamer and piperazine-polyethylenimine derivative for targeted siRNA delivery into breast cancer cells, *Int. J. Pharm.* 485 (2015) 50–60. <https://doi.org/10.1016/J.IJPHARM.2015.02.031>.
 - [18] H.J. Zhang, X. Zhao, L.J. Chen, C.X. Yang, X.P. Yan, Dendrimer grafted persistent luminescent nanoplatfrom for aptamer guided tumor imaging and acid-responsive drug

- delivery, *Talanta*. 219 (2020) 121209. <https://doi.org/10.1016/j.talanta.2020.121209>.
- [19] Y. Wang, C. Zhou, Y. Ding, M. Liu, Z. Tai, Q. Jin, Y. Yang, Z. Li, M. Yang, W. Gong, C. Gao, Red blood cell-hitchhiking chitosan nanoparticles for prolonged blood circulation time of vitamin K1, *Int. J. Pharm.* 592 (2021) 120084. <https://doi.org/10.1016/j.ijpharm.2020.120084>.
- [20] Y. Guo, D. Wang, Q. Song, T. Wu, X. Zhuang, Y. Bao, M. Kong, Y. Qi, S. Tan, Z. Zhang, Erythrocyte Membrane-Enveloped Polymeric Nanoparticles as Nanovaccine for Induction of Antitumor Immunity against Melanoma, *ACS Nano*. 9 (2015) 6918–6933. <https://doi.org/10.1021/acs.nano.5b01042>.
- [21] P. Kesharwani, L. Xie, S. Banerjee, G. Mao, S. Padhye, F.H. Sarkar, A.K. Iyer, Hyaluronic acid-conjugated polyamidoamine dendrimers for targeted delivery of 3,4-difluorobenzylidene curcumin to CD44 overexpressing pancreatic cancer cells., *Colloids Surf. B. Biointerfaces*. 136 (2015) 413–423. <https://doi.org/10.1016/j.colsurfb.2015.09.043>.
- [22] M. Shahriari, S.M. Taghdisi, K. Abnous, M. Ramezani, M. Alibolandi, Synthesis of hyaluronic acid-based polymersomes for doxorubicin delivery to metastatic breast cancer, *Int. J. Pharm.* 572 (2019) 118835. <https://doi.org/10.1016/j.ijpharm.2019.118835>.
- [23] C.M. Pinto, L.S. Horta, A.P. Soares, B.A. Carvalho, E. Ferreira, E.B. Lages, L.A.M. Ferreira, A.A.G. Faraco, H.C. Santiago, G.A.C. Goulart, Nanoencapsulated doxorubicin prevents mucositis development in mice, *Pharmaceutics*. 13 (2021). <https://doi.org/10.3390/pharmaceutics13071021>.
- [24] J. Zhu, Z. Xiong, M. Shen, X. Shi, Encapsulation of doxorubicin within multifunctional gadolinium-loaded dendrimer nanocomplexes for targeted theranostics of cancer cells, *RSC Adv.* 5 (2015) 30286–30296. <https://doi.org/10.1039/c5ra01215e>.
- [25] A. Rudra, R.M. Deepa, M.K. Ghosh, S. Ghosh, B. Mukherjee, Doxorubicin-loaded phosphatidylethanolamine-conjugated nanoliposomes: in vitro characterization and their accumulation in liver, kidneys, and lungs in rats, *Int. J. Nanomedicine*. 5 (2010) 811–823. <https://doi.org/10.2147/IJN.S13031>.
- [26] S. Li, Y. Ma, X. Yue, Z. Cao, Z. Dai, One-pot construction of doxorubicin conjugated magnetic silica nanoparticles, *New J. Chem.* 33 (2009) 2414–2418. <https://doi.org/10.1039/B9NJ00342H>.
- [27] D.H. Nguyen, L.G. Bach, D.H.N. Tran, V. Du Cao, T.N.Q. Nguyen, T.T.H. Le, T.T. Tran, T.T.H. Thi, Partial surface modification of low generation polyamidoamine dendrimers: Gaining insight into their potential for improved carboplatin delivery, *Biomolecules*. 9 (2019) 1–16. <https://doi.org/10.3390/biom9060214>.
- [28] I. Khan, G. Joshi, K.T. Nakhate, Ajazuddin, R. Kumar, U. Gupta, Nano-Co-Delivery of Berberine and Anticancer Drug Using PLGA Nanoparticles: Exploration of Better Anticancer Activity and In Vivo Kinetics, *Pharm. Res.* 36 (2019). <https://doi.org/10.1007/s11095-019-2677-5>.
- [29] M. Alibolandi, F. Hoseini, M. Mohammadi, P. Ramezani, E. Einafshar, S.M. Taghdisi, M. Ramezani, K. Abnous, Curcumin-entrapped MUC-1 aptamer targeted dendrimer-gold hybrid nanostructure as a theranostic system for colon adenocarcinoma, *Int. J. Pharm.* 549 (2018) 67–75. <https://doi.org/10.1016/j.ijpharm.2018.07.052>.
- [30] M. Alibolandi, M. Ramezani, F. Sadeghi, K. Abnous, F. Hadizadeh, Epithelial cell adhesion molecule aptamer conjugated PEG-PLGA nanopolymersomes for targeted delivery of doxorubicin to human breast adenocarcinoma cell line in vitro., *Int. J. Pharm.* 479 (2015) 241–51. <https://doi.org/10.1016/j.ijpharm.2014.12.035>.
- [31] P. Kesharwani, L. Xie, G. Mao, S. Padhye, A.K. Iyer, Hyaluronic acid-conjugated polyamidoamine dendrimers for targeted delivery of 3,4-difluorobenzylidene curcumin

- to CD44 overexpressing pancreatic cancer cells, 136 (2015) 413–423. <https://doi.org/10.1016/j.colsurfb.2015.09.043>.
- [32] M. Alibolandi, M. Ramezani, K. Abnous, F. Hadizadeh, AS1411 Aptamer-Decorated Biodegradable Polyethylene Glycol–Poly(lactic-co-glycolic acid) Nanopolymersomes for the Targeted Delivery of Gemcitabine to Non–Small Cell Lung Cancer In Vitro, J. Pharm. Sci. 105 (2016) 1741–1750. <https://doi.org/10.1016/J.XPHS.2016.02.021>.
- [33] M. Falsafi, M. Zahiri, A.S. Saljooghi, K. Abnous, S.M. Taghdisi, A. Sazgarnia, M. Ramezani, M. Alibolandi, Aptamer targeted red blood cell membrane-coated porphyrinic copper-based MOF for guided photochemotherapy against metastatic breast cancer, Microporous Mesoporous Mater. 325 (2021) 111337. <https://doi.org/10.1016/j.micromeso.2021.111337>.
- [34] A. Barzegar Behrooz, F. Nabavizadeh, J. Adiban, M. Shafiee Ardestani, R. Vahabpour, M.R. Aghasadeghi, H. Sohanaki, Smart bomb AS1411 aptamer-functionalized/PAMAM dendrimer nanocarriers for targeted drug delivery in the treatment of gastric cancer, Clin. Exp. Pharmacol. Physiol. 44 (2017) 41–51. <https://doi.org/10.1111/1440-1681.12670>.
- [35] X. Xu, L. Li, X. Li, D. Tao, P. Zhang, J. Gong, Aptamer-protamine-siRNA nanoparticles in targeted therapy of ErbB3 positive breast cancer cells, Int. J. Pharm. 590 (2020). <https://doi.org/10.1016/j.ijpharm.2020.119963>.
- [36] M. Mohammadi, L. Arabi, M. Alibolandi, Doxorubicin-loaded composite nanogels for cancer treatment, J. Control. Release. 328 (2020) 171–191. <https://doi.org/10.1016/j.jconrel.2020.08.033>.



Dr. Prashant Kesharwani

Date: 21 Aug. 23